Bidirectional Chemo-Switching of Spin State in a Microporous Framework**

Masaaki Ohba, Ko Yoneda, Gloria Agustí, M. Carmen Muñoz, Ana B. Gaspar, José A. Real,**
*Mikio Yamasaki, Hideo Ando, Yoshihide Nakao, Shigeyoshi Sakaki, and Susumu Kitagawa**

Porous coordination polymers (PCPs) have appeared in the past decade as a new class of porous materials providing permanent and designable regular microporosity through flexible coordination bonds.[1–4] Compared with existing inorganic porous materials, PCPs provide significant enhancement in flexibility and in the dynamics of their frameworks.[4] This versatility has created prospects for applications in gas storage, gas separation, and heterogeneous catalysis. The next generation of PCPs is being conceived to switch various solid-state properties (e.g., optics, conductivity, or magnetism) through guest adsorption processes, which resemble, in a simplified form, the conversion process from chemical stimulus to information signal in the chemosensory organs for taste and smell. Herein, the chemical response of the framework would be crucial for producing drastic physico-chemical changes. To implement such chemoresponsive switching at ordinary temperatures we focused on coupling the porous properties and the spin-crossover (SCO) phenomenon. SCO is well known in iron(II) coordination compounds, whose electron configurations can move between high-spin (HS) and low-spin (LS) states under external perturbations (temperature, pressure, and light irradiation), producing changes in magnetic, optical, dielectric, and structural properties.[5–10] In special cases, this switch can be performed within the hysteresis loop based on the first-order spin transition (ST). Although several compounds have been reported as PCPs incorporating SCO subunits (SCO–PCPs), these materials do not display a room temperature first-order hysteretic spin transition,[10] the guest adsorption and SCO being essentially disconnected events. In these SCO–PCPs, adsorption of guest molecules induces an incomplete and gradual spin transition at low temperature. Even now, strategies for the direct coupling of porous properties and magnetic switching are still underdeveloped.

To establish a new approach to guest-responsive SCO, we adopted Hofmann-type three-dimensional (3D) SCO–PCPs, $\{Fe(pz)[M^{II}(CN)_4]\}$ (pz = pyrazine; M^{II} = Ni, Pd, Pt)[6c] as a platform. These compounds display cooperative magnetic and chromatic thermal- and light-induced spin transition in the region of room temperature.[7] In particular, $\{Fe(pz)[Pt(CN)_4]\}$ (**1**) displays a first-order spin transition with approximately 25 K wide hysteresis (critical temperatures: $T_c^{\downarrow} = 285$ K and $T_c^{\uparrow} = 309$ K), and its SCO properties are retained in a thin film[7b,c] or nanocrystals.[8] Based on ab initio X-ray powder diffraction results of dihydrated **1** (**1**·2 H$_2$O), we found that the framework provides two guest-interactive sites, one between the pz-bridges (site A) and another between the four-coordinate Pt centers (site B). Furthermore, the pz-bridges are provided with rotational freedom in the framework. These features should be important for the chemical response of the framework.

Herein we report chemoresponsive bidirectional spin-state switching in **1** in the room temperature bistability region. Compound **1** can allow reversible control of the magnetic and optical outputs through the chemical response of the framework, as one of a new generation of functional materials responding to their environment. The key factors for the guest-responsive ST were highlighted by theoretical calculations.

Typically, **1** is found in its dihydrate form **1**·2 H$_2$O. The structures of **1**·2 H$_2$O in the HS and LS states were determined using the same single crystal at 293 K (See Supporting

[*] Dr. M. Ohba, K. Yoneda, Prof. Dr. S. Kitagawa
Department of Synthetic Chemistry and Biological Chemistry,
Graduate School of Engineering, Kyoto University
Katsura, Nishikyo-ku, Kyoto 615-8510 (Japan)
Fax: (+81) 75-383-2732
E-mail: ohba@sbchem.kyoto-u.ac.jp
        kitagawa@sbchem.kyoto-u.ac.jp

G. Agustí, Dr. A. B. Gaspar, Prof. Dr. J. A. Real
Institut de Ciència Molecular, ICMOL/Departament de Química
Inorgánica, Universitat de València, Edifici d'Instituts de Paterna
Apartat de correus 22085, 46071 València (Spain)
E-mail: jose.a.real@uv.es

Prof. Dr. M. C. Muñoz
Departament de Física Aplicada, Universitat Politècnica de València
Camí de Vera s/n, 46022 València (Spain)

Dr. M. Yamasaki
Rigaku Corporation
Matsubaracho, Akishima, Tokyo 196-8666 (Japan)

H. Ando, Dr. Y. Nakao, Prof. Dr. S. Sakaki
Department of Molecular Engineering, Graduate School of Engineering, Kyoto University
Katsura, Nishikyo-ku, Kyoto 615-8510 (Japan)

Dr. M. Ohba, Prof. Dr. S. Kitagawa
RIKEN Spring-8 Center
Kouto, Sayo-cho, Sayo-gun, Hyogo 679-5198 (Japan)

Prof. Dr. S. Kitagawa
Institute for Integrated Cell-Material Sciences (iCeMS), Kyoto University
Konoe-cho, Yoshida, Sakyo-ku, Kyoto 606-8501 (Japan)

Information), where the HS and LS states were stabilized by cooling from 340 K to 293 K and by heating from 240 K to 293 K, respectively. In both states, each square-planar $[Pt(CN)_4]^{2-}$ anion connects four adjacent axially distorted octahedral Fe^{II} atoms (Figure 1 a,b). The equatorial positions

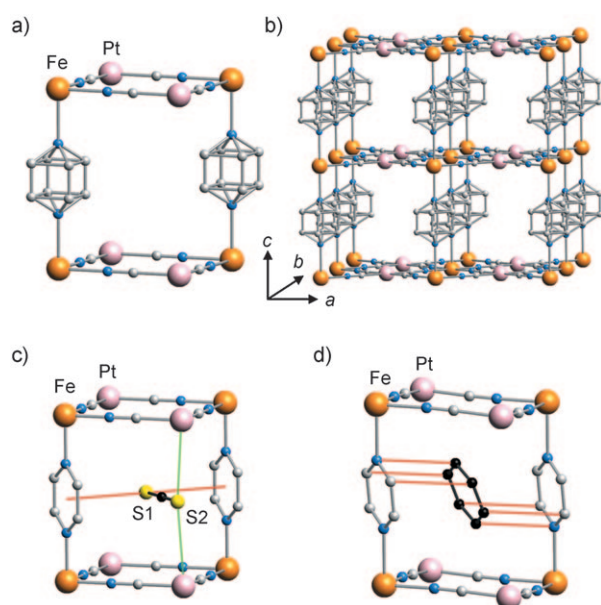***Figure 1.*** Crystal structures of {Fe(pz)[Pt(CN)$_4$]·2 H$_2$O} (**1**·2 H$_2$O) and CS$_2$ and pyrazine clathrates (**1**·CS$_2$ and **1**·pz). a) The basic cavity structure of **1**·2 H$_2$O. b) Projection of the 3D porous framework of **1**·2 H$_2$O. c) The basic cavity structure of **1**·CS$_2$. The S2 atom is disordered through the mirror plane on the S1 atom, and one S2 atom is omitted for clarifying. d) The basic cavity structure of **1**·pz. Fe (orange), Pt (pink), N (blue), C (gray), S (yellow), guest molecules (black except for S atoms); the red and green lines in (c) and (d) are a guide for the eye and indicate the closest contacts between the guest and the framework.

of the iron center are occupied by the four cyano nitrogen atoms of the $[Pt(CN)_4]^{2-}$ anions. In the lattice, a 2D $\{Fe[Pt(CN)_4]\}_\infty$ grid is formed by the Pt-CN-Fe linkages on the (001) plane with Fe$_2$Pt$_2$ square windows. The bridging pyrazine ligands occupy the remaining apical positions of the Fe octahedrons and act as pillars (collinear to the C_4 axis) connecting consecutive layers along the (001) direction (Figure 1b), and it forms channels with a gate size of 3.92 × 4.22 Å^2 for the HS state and 3.43 × 3.94 Å^2 for the LS state, parallel to the (100) and (010) directions (Supporting Information, Figure S2). The equatorial and axial Fe–N bond lengths at 293 K are 2.148(6) and 2.215(15) Å for the HS state and 1.941(7) and 1.985(16) Å for the LS state. Upon the spin transition, the unit cell volume changes by 53.5(5) Å^3 per Fe atom. The solvent-accessible voids of the LS state and HS state were estimated to be 18.1 and 22.4%, respectively.

The guest-free framework of **1** adsorbs various guest molecules in the gas phase or solution and forms their clathrates. X-ray diffraction measurements of the CS$_2$ clathrate (**1**·CS$_2$) were performed at 93 K to minimize thermal vibration (Figure 1c). The equatorial and axial Fe–N bond lengths are typical of the LS state, at 1.927(7) and 1.971(9) Å,

respectively. The CS$_2$ molecules lie in the middle of the channels running along the (010) direction, and there is no direct contact between the CS$_2$ molecule and the Fe center (Fe···S1 = 4.921 Å and Fe···S2 = 5.797 Å). The S1 atom interposes between the pz rings (site A) with a separation from the center of the pz ring of 3.588 Å. The S2 atom sits over the Pt atoms (site B) with a separation of 3.405 Å. The S1 atom is located on the mirror plane, and the S2 atom lies on two sites with an occupancy of 0.5. In the case of the pyrazine clathrate (**1**·pz), the guest pyrazine molecule lies in site A and leans toward the pz pillars with three-point π···π contacts (3.425–3.546 Å; Figure 1d). The Fe–N bond lengths correspond well with those of the HS state (equatorial, 2.128(12) Å; axial, 2.252(14) Å). When the crystals of **1**·CS$_2$ and **1**·pz are heated, the guest-free framework **1** is formed as the result of a single-crystal-to-single-crystal transformation. The thus prepared guest-free crystals of **1** in the LS and HS states determined at 293 K display the original spin-transition behavior observed in **1**.

The adsorption isotherm of benzene using **1**-LS shows a step rise at a very low P/P_0 value (ca. 0.05) with saturation accompanied by a color change (See Supporting Information). The benzene clathrate (**1**·bz) is paramagnetic at all temperatures (Figure 2a). In situ observation of the benzene-induced spin transition at 293 K was monitored directly using a sample holder specially designed to introduce vapor into the SQUID magnetometer (Figure 2b). A complete and relatively rapid conversion from the LS state (**1**-LS) to the HS state (**1**·bz) is observed (Figure 2b) for $P/P_0 = 0.19$. Desorption of benzene under vacuum produces the unclathrated framework **1**-HS. The system does not recover the initial LS state over a period of months after releasing benzene within the bistable temperature region. This memory function retains information about adsorption of the guest molecules in the form of the spin state, magnetism, color, and structure, information that can be erased by desorption and cooling (Scheme 1). X-ray powder diffraction of **1**·bz suggested essentially the same structure as for **1**·pz, which shows the same magnetic behavior as **1**·bz. Other six- or five-membered aromatic molecules, such as pyrazine, pyridine, thiophene, pyrrole, and furan, or solvents, such as methanol, ethanol, propanol, and tetrahydrofuran, display a similar behavior to that shown by benzene at room temperature (Table 1). In all of these examples, **1**-HS is stabilized after inclusion of the guests within the hysteresis loop of **1**.

In contrast, **1**-HS promptly adsorbs one molecule of CS$_2$ for $P/P_0 < 0.1$ and simultaneously changes to the LS state leading to **1**·CS$_2$ (Figure 2b). The magnetic change rate is faster than that of **1**·bz, which means a higher affinity of CS$_2$ for the framework than that of benzene. Indeed, injection of CS$_2$ vapor onto **1**·bz induces a gradual and complete replacement of benzene by CS$_2$ even under a saturated benzene vapor atmosphere. **1**·CS$_2$ maintains the LS state without spin transition in the temperature range 2–330 K (Figure 2a); above 330 K the $\chi_M T$ value increases because of the release of CS$_2$. When the CS$_2$ molecule is removed at 298 K under vacuum, the framework retains the LS state as a result of the memory effect described above (Scheme 1). Benzene adsorption resulted in expansion (softening) of the framework with a
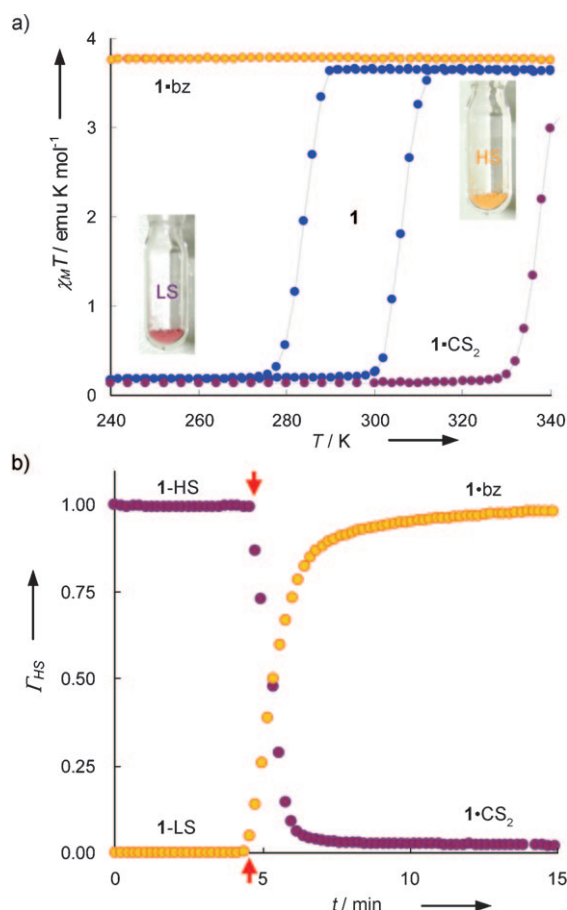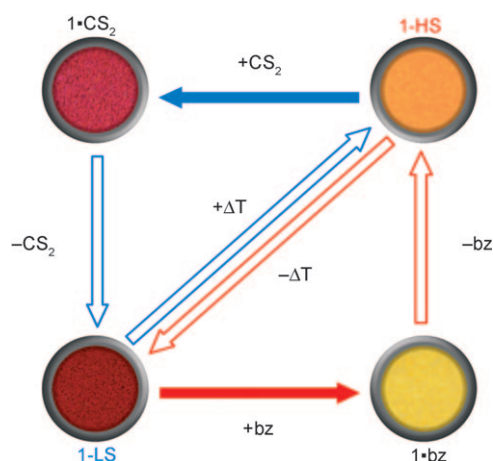
Figure 2. Magnetic behaviors of **1** and its clathrates and in situ observation of the guest-induced spin transition. a) Temperature dependences of $\chi_M T$ for guest-free **1** (blue), benzene clathrate (**1**·bz: yellow), and CS_2 clathrate (**1**·CS_2: purple) in the temperature range 240–340 K. The sample color changed between deep red (LS) and yellow-orange (HS) depending on the temperature and guest molecules. b) Time dependence of the fraction of the HS state (Γ) under a benzene (yellow) and CS_2 (purple) atmosphere at 293 K. Red arrows indicate the starting points of guest injection (valve opening).

Scheme 1. Schematic chemical and thermal memory process. The color circles are photos of samples. Adsorption of benzene induces the HS state from **1**-LS (red solid arrow). The recorded HS state is retained after desorption of benzene under vacuum and then returned to the initial LS state by cooling (red outlined arrows). Conversely, CS_2 produces the LS state from **1**-HS with contraction of the framework as a recorded state (blue solid arrow). The recorded LS state is initialized by successive desorption of CS_2 under vacuum and heating (blue outlined arrows).

Table 1: Summary of the guest induced spin state of **1** at 293 K.

Class	Guest molecule		Effect
I	CO_2, O_2	N_2,	None
II	H_2O, MeOH, 2-PrOH, Benzene, Toluene, Pyrrole, Furan,	D_2O, EtOH, Acetone, Pyrazine, Pyridine, Thiophene, THF	HS stabilized
III	CS_2		LS stabilized

LS-to-HS transition; in stark contrast, CS_2 adsorption contracted (hardened) the framework accompanying an HS-to-LS transition. The analogues of {Fe(pz)[M(CN)$_4$]} (M = Ni, Pd) demonstrate similar guest-responsive spin-state switching. In the case of the gas molecules, CO_2, O_2, and N_2, only CO_2 is adsorbed at 298 K, but shows no spin-state change (see Supporting Information).

The studied guest molecules (G) can be grouped into three major classes according to their effect on the spin state (Table 1). Class I (gas molecules: N_2, O_2, and CO_2) showed no effect on the spin state; class II (H_2O, alcohols, acetone, and five- or six-membered ring molecules) stabilized the HS state; and class III (CS_2) stabilized the LS state. The structural characteristics of the clathrates are as follows: 1) the CS_2 molecules are located at sites A and B; and 2) the pz guest molecules are located exclusively at site A preventing further contraction of the framework to the LS state. These structural results, together with guest classification, point to three key factors as the origins of the relative stabilities of the HS and LS states: 1) the size and shape of the guest (G); 2) the G···pz interaction at site A; and 3) the G···Pt interaction at site B.

To corroborate the exceptional response of the framework to CS_2, binding energies between CS_2 and each site (A and B) were estimated (Figure 3 and Supporting Information). Although potential energy surfaces calculated with the density functional theory (DFT) and the Hartree–Fock (HF) methods showed no binding between S and each site, the highly accurate CCSD(T) method with the counterpoise correction[11] gave binding energies of approximately 4.2 kcal mol^{-1} at site A (Figure 3a) and approximately 5.5 kcal mol^{-1} at site B (Figure 3b), indicating that van der Waals interactions rather than charge-transfer interactions mainly contribute. The van der Waals interactions make the guest molecule take the midpoint between two pz bridges. In the case of isomorphic CO_2 molecules (class I), they indicate a weak interaction (ca. 2.9 kcal mol^{-1} at site A; ca. 4.2 kcal mol^{-1} at site B). These computational results highlight the significant interaction of CS_2 at sites A and B. In future work, the
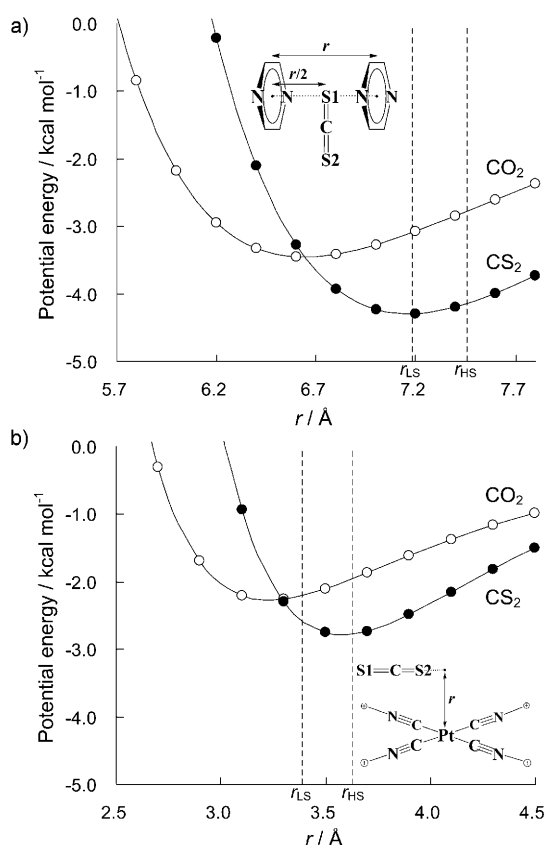
a)

b)

Figure 3. Potential energy curves for the interaction of CS_2 and CO_2 at a) site A and b) sit B. r_{LS} and r_{HS} represent the corresponding distances in the experimental $1 \cdot 2\,H_2O(LS)$ and $1 \cdot 2\,H_2O(HS)$ frameworks, respectively. The binding energies of CS_2 and CO_2 at site B discussed in the text are estimated as double the value in Figure 3 b, because the molecules interact with two Pt at site B.

rotation of pyrazine bridges, the change of crystallogpraphic symmetry, and the change of π-acceptor character of the cyanide groups will be verified as potential factors for stabilization of the LS state. In contrast, for class II, the number of guests per iron atom, guest size, and shape determine the stabilization of the HS state. Steric hindrance prevents further contraction of the clathrates' framework, resulting in an inhibition of the HS-to-LS transition or a notable displacement of $T_c^{\downarrow}$ to lower temperatures.

In summary, an unprecedented bidirectional chemo-switching is delivered using the dynamic microporous SCO–PCP {Fe(pz)[Pt(CN)$_4$]} (**1**) at room temperature. The HS and LS states are reversibly induced with coupling of guest adsorption (Scheme 1). The space inside the framework of **1** allows a chemical response for sites A and B. The CS_2 molecule interacts with sites A and B and exceptionally stabilizes the LS state. The singularity of the framework response for CS_2 is corroborated by theoretical calculations. The SCO–PCP **1** presents bidirectional chemo-switching of spin state and memory effect at room temperature, which will open a route for evolving the PCPs to environmentally responsive materials; for example, nano-sized chemical memories and chemical sensors.

Experimental Section

Single crystals of clathrates were prepared by slow diffusion of a methanolic solution of guest molecules and K$_2$[Pt(CN)$_4$] to an aqueous solution containing [Fe(SO$_4$)$_2$(NH$_4$)$_2$]·6 H$_2$O and pz.

Variable-temperature X-ray powder diffraction was carried out on a Rigaku RINT-2000 Ultima diffractometer with Cu$_{K\alpha}$ radiation. Thermogravimetric analyses were recorded on a Rigaku Thermo plus TG 8120 apparatus in the temperature range between 300 and 700 K under a nitrogen atmosphere at a heating rate of 1 K min^{-1}. The adsorption isotherms of CO_2, O_2, and N_2 were measured with Quantachrome AUTOSORB-1 and adsorption/desorption isotherms for H_2O and benzene at 298 K were measured with BELSORP-18 volumetric adsorption equipment from BEL Japan, Inc. The anhydrous sample **1** was obtained by treatment under reduced pressure ($<10^{-2}$ Pa) at 400 K for more than 2 h.

Magnetic susceptibilities of all samples were measured on a Quantum Design MPMS-XL5R SQUID susceptometer in the temperature range 2–300 K in an applied dc field of 500 Oe. The samples were placed in a glass tube and fixed to the end of the sample transport rod. Guest-free sample was prepared by evacuating the SQUID sample chamber at 293 K for 2 h. The guest molecules were injected through the long metallic rod of the sample holder ending in a hermetically closed cylindrical chamber with vapor-pressure control at 293 K. The molar magnetic susceptibility, χ_M, was corrected for the diamagnetism of the constituent atoms.

X-ray diffraction data of $1 \cdot 2\,H_2O(HS)$, $1 \cdot 2\,H_2O(LS)$, $1 \cdot CS_2$, **1**-HS, and **1**-LS were collected on a Rigaku Varimax CCD system, **1**·pz was collected with a Nonius Kappa-CCD single-crystal diffractometer. In all cases, graphite-monochromated Mo$_{K\alpha}$ radiation ($\lambda = 0.71070$ Å) was used. A single crystal was mounted on a fiber loop with liquid paraffin and the temperature kept constant under flowing N$_2$. All of the structures were solved by a standard direct method (Crystal Clear 1.4. crystallographic software package of the Molecular Structure Corp. and Rigaku) and expanded using Fourier techniques. Full-matrix least-squares refinements were carried out with anisotropic thermal parameters for all non-hydrogen atoms. All of the hydrogen atoms were placed in the calculated positions and refined using a riding model. CCDC 660920 ($1 \cdot 2\,H_2O(HS)$), 660921 ($1 \cdot 2\,H_2O(LS)$), 660922 ($1 \cdot CS_2$), 660923 (**1**-HS), 660924 (**1**-LS), 684312 (**1**·pz) contain the supplementary crystallographic data for this paper. These data can be obtained free of charge from The Cambridge Crystallographic Data Centre via www.ccdc.cam.ac.uk/data_request/cif.

[1] a) G. Férey, C. Mellot-Draznieks, C. Serre, F. Millange, *Acc. Chem. Res.* **2005**, *38*, 217–225; b) N. W. Ockwig, O. Delgado-Friedrichs, M. O'keeffe, O. M. Yaghi, *Acc. Chem. Res.* **2005**, *38*, 176; c) S. Kitagawa, R. Kitaura, S. Noro, *Angew. Chem.* **2004**, *116*, 2388–2430; *Angew. Chem. Int. Ed.* **2004**, *43*, 2334–2375; d) M. J. Rosseinsky, *Microporous Mesoporous Mater.* **2004**, *73*, 15–30; e) C. Janiak, *Dalton Trans.* **2003**, 2781–2804; f) G. S. Papaefstathiou, L. R. MacGillivary, *Coord. Chem. Rev.* **2003**, *246*, 169–184; g) B. Moulton, M. J. Zaworotko, *Chem. Rev.* **2001**, *101*, 1629.

[2] a) G. Férey, C. Mellot-Draznieks, C. Serre, F. Millange, J. Dutour, S. Surblé, I. Margiolaki, *Science* **2005**, *309*, 2040–2042; b) R. Matsuda, R. Kitaura, S. Kitagawa, Y. Kubota, R. V. Belosludov, T. C. Kobayashi, H. Sakamoto, T. Chiba, M. Takata, Y. Kawazoe, Y. Mita, *Nature* **2005**, *436*, 238–241; c) O. M. Yaghi, M. O'Keeffe, N. W. Ockwig, H. K. Chae, M.

Eddaoudi, J. Kim, *Nature* **2003**, *423*, 705 – 714; d) M. Eddaoudi, J. Kim, N. Rosi, D. Vodak, J. Wachter, M. O'keeffe, O. M. Yaghi, *Science* **2002**, *295*, 469 – 472; e) J. S. Seo, D. Whang, H. Lee, S. I. Jun, J. Oh, Y. J. Jeon, K. Kim, *Nature* **2000**, *404*, 982 – 986.

[3] a) D. Maspoch, S. R. Molina, J. Veciana, *Chem. Soc. Rev.* **2007**, *36*, 770 – 818; b) N. Yanai, W. Kaneko, K. Yoneda, M. Ohba, S. Kitagawa, *J. Am. Chem. Soc.* **2007**, *129*, 3496 – 3497; c) C. J. Kepert, *Chem. Commun.* **2006**, 696 – 700; d) S. Ohkoshi, K. Arai, Y. Sato, K. Hashimoto, *Nat. Mater.* **2004**, *3*, 857 – 861; e) D. Maspoch, D. R. Molina, K. Wurst, N. Domingo, M. Cavallini, F. Biscarini, J. Tejada, C. Rovira, J. Veciana, *Nat. Mater.* **2003**, *2*, 190 – 195.

[4] a) S. Kitagawa, R. Matsuda, *Coord. Chem. Rev.* **2007**, *251*, 2490 – 2509; b) S. Horike, R. Matsuda, D. Tanaka, S. Matsubara, M. Mizuno, K. Endo, S. Kitagawa, *Angew. Chem.* **2006**, *118*, 7384 – 7388; *Angew. Chem. Int. Ed.* **2006**, *45*, 7226 – 7230.

[5] a) "Spin Crossover in Transition Metal Compounds" (Eds.: P. Gütlich, H. A. Goodwin): *Top. Curr. Chem.* **2004**, *233–235*; b) O. Kahn, C. J. Martines, *Science* **1998**, *279*, 44 – 48.

[6] a) J. A. Real, A. B. Gaspar, M. C. Muñoz, *Dalton Trans.* **2005**, 2062; b) J. A. Real, A. B. Gaspar, V. Niel, M. C. Muñoz, *Coord. Chem. Rev.* **2003**, *236*, 121 – 141; c) V. Niel, J. M. Martinez-Agudo, M. C. Muñoz, A. B. Gaspar, J. A. Real, *Inorg. Chem.* **2001**, *40*, 3838.

[7] a) S. Cobo, D. Ostrovskii, S. Bonhommeau, L. Vendier, G. Molnàir, L. Salmon, K. Tanaka, A. Bousseksou, *J. Am. Chem. Soc.* **2008**, *130*, 9019 – 9024; b) G. Molnár, S. Cobo, J. A. Real, F. Carcenac, E. Daran, C. Vieu, A. Bousseksou, *Adv. Mater.* **2007**, *19*, 2163; c) S. Bonhommeau, G. Molnár, A. Galet, A. Zwick, J. A. Real, J. J. McGarvey, A. Bousseksou, *Angew. Chem.* **2005**, *117*, 4137 – 4141; *Angew. Chem. Int. Ed.* **2005**, *44*, 4069 – 4073; d) T. Tayagaki, A. Galet, G. Molnár, M. C. Muñoz, A. Zwick, K. Tanaka, J. A. Real, A. Bousseksou, *J. Phys. Chem. B* **2005**, *109*, 14859.

[8] a) I. Boldog, A. B. Gaspar, V. Martínez, P. Pardo-Ibáñez, V. Ksenofontov, A. Bhattacharjee, P. Gütlich, J. A. Real, *Angew. Chem.* **2008**, *120*, 6533 – 6537; *Angew. Chem. Int. Ed.* **2008**, *47*, 6433 – 6437; b) F. Volatron, L. Catala, E. Rivielre, A. Gloter, O. Steìphan, T. Mallah, *Inorg. Chem.* **2008**, *47*, 6584 – 6586.

[9] a) P. Gütlich, A. Hauser, H. Spiering, *Angew. Chem.* **1994**, *106*, 2109 – 2141; *Angew. Chem. Int. Ed.* **1994**, *33*, 2024 – 2054; b) A. Hauser, J. Jeftic, H. Romstedt, R. Hinek, H. Spiering, *Coord. Chem. Rev.* **1999**, *190–192*, 471 – 491; c) S. Decurtins, P. Gütlich, C. P. Köhler, H. Spiering, A. Hauser, *Chem. Phys. Lett.* **1984**, *105*, 1 – 4.

[10] a) J. A. Real, E. Andrés, M. C. Muñoz, M. Julve, T. Granier, A. Bousseksou, F. Varret, *Science* **1995**, *268*, 265 – 267; b) G. J. Halder, C. J. Kepert, B. Moubaraki, K. S. Murray, J. D. Cashion, *Science* **2002**, *298*, 1762 – 1765; c) S. M. Neville, G. J. Halder, K. W. Chapman, M. B. Duriska, P. D. Southon, J. D. Cashion, J. F. Létard, B. Moubaraki, K. S. Murray, C. J. Kepert, *J. Am. Chem. Soc.* **2008**, *130*, 2869 – 2876.

[11] S. F. Boys, F. Bernardi, *Mol. Phys.* **1970**, *19*, 553 – 566.